Singlet and Triplet Exciton Dynamics of Violanthrone

Elham M. Gholizadeh[1], Shyamal K. K. Prasad[1], Lara Gillan[2],
Dane R. McCamey[2], Murad J. Y. Tayebjee[3] and Timothy W. Schmidt[1*]

[1]ARC Centre of Excellence in Exciton Science,
School of Chemistry, UNSW Sydney, NSW 2052, Australia
[2]ARC Centre of Excellence in Exciton Science,
School of Physics, UNSW Sydney, NSW 2052, Australia
[3]School of Photovoltaic and Renewable Energy Engineering, UNSW Sydney, NSW 2052, Australia

[*]To whom correspondence should be addressed; E-mail: timothy.schmidt@unsw.edu.au.

Abstract

The exciton dynamics of violanthrone-79 are investigated in solution and in the solid state. In solution, the photo-prepared singlet is found to exhibit a strong ground-state bleach and stimulated emission feature, but when sensitized in its triplet state, exhibits only a narrow and weak ground-state bleach. As supported by density functional theory calculations, this is explained by the triplet state having absorptions in the same region, with a similar oscillator strength, as the ground state molecule. In solid films, the excited singlet is found to survive only $100\,ps$, giving way to a long-lived transient absorption spectrum with characteristics reminiscent of the triplet in solution. This is interpreted in terms of singlet fission in the solid film.

Excitonic interactions involving the interplay of excited singlet excitons and pairs of triplet excitons in organic semiconductors have the potential to transform a number of technologies, including solar photovoltaics,[1–7] photocatalysis,[8, 9] photodynamic therapy,[10] and biological imaging.[11] The conversion of triplet excitons generated with low energy photons into a higher energy singlet excitons is known as triplet fusion, or photochemical upconversion.[1, 8, 12–15] The excitonic interaction at play, triplet-triplet annihilation, is the conjugate process to

1

singlet fission.[16, 17] In singlet fission, a high-energy singlet state splits into two lower-energy triplet states, with the latter being available for energy harvesting.[3, 4, 18–21] As such, in a photovoltaic device, high energy photons generate double the photocurrent of lower energy photons, raising the efficiency limit from 33.7 % to 45.9 % under one sun illumination.[22]

To explore the low-energy limits of triplet fusion, chromophores with low-lying triplets are required. Recently, we demonstrated that the dye violanthrone-79 (V79) could be used as an annihilator to achieve photochemical upconversion from below the silicon band gap.[23, 24] However, implementing this as a solid state technology is hindered by the poor performance of V79 in the solid state where it has a very low fluorescence yield. The related molecule, violanthrone-78, is known to have an excited-state lifetime in the solid state as short as 20 ps, and exhibits J-like excitonic coupling.[25] This short lifetime may be due to singlet fission, as the triplet level of V79 is known to be below 0.98 eV, and the 0-0 emission is at 1.85 eV.[24] There is precedence for endothermic fission in films of molecules used for triplet fusion in solution. Rubrene, a well-known annihilator used in triplet-triplet annihilation, is known to undergo endothermic singlet fission in the condensed phase, preventing high triplet fusion yields. Doping the material to trap the excited singlet state has been employed to circumvent this problem.[26] However, the details of crystal structure can also play a role in preventing fission.[27]

In this study, we explore the exciton dynamics of V79 using transient absorption spectroscopy, first in solution, and then in a film. The solution triplet state spectrum is revealed by sensitization with platinum octaethylporphyrin (PtOEP). The transient spectrum of a film of V79 reveals a short-lived excited state which gives rise to a longer-lived state. We interpret this behaviour in terms of singlet fission, guided by density functional theory calculations.

1 Experimental Methods

1.1 Sample Preparation

Solutions were made in toluene in a 1 mm-pathlength cuvette. V79 was prepared at a maximum optical density of 0.3 (0.1 mM, $\epsilon_{635} = 27600 \text{M}^{-1}\text{cm}^{-1}$). The peak optical densities of V79 and PtOEP ($\epsilon_{536} = 63760 \text{M}^{-1}\text{cm}^{-1}$[28]) in the mixture were 0.8 and 0.7 respectively (0.3 mM and 0.1 mM). The V79 film was prepared by drop-casting a solution of V79 in toluene onto a glass slide.

1.2 Spectroscopy

Transient absorption spectroscopy was performed using a home-built set-up. The probe pulse was generated by focusing the 785 nm pulse (1000 Hz, Clark-MXR CPA 2210, 150 fs, Ti:sapph. regen. amp.) onto an yttrium aluminium garnet crystal. The subsequent supercontinuum was dispersed by a home-built prism spectrometer, thus allowing simultaneous collection across the visible and near-infrared regions. For fs-ns time-scales, the pump pulse was generated by a 2-stage optical parametric amplifier (TOPAS-C, light conversion). The pump pulses were delayed using a motorized delay stage (Thorlabs, LTS300). An optical chopper modulated the pump laser, blocking every second pulse. For longer >ns time-scales, the pump pulse was generated with the 532 nm output of a 800 ps pulse-width Nd:YAG laser (InnoLas picolo), with the timing controlled electronically.

The supercontinuum spectrum (probe) and pump pulse energy was measured on a shot-to-shot basis. The probe spectrum was converted to differential transmission by comparison of the shots collected respectively with and without the pump pulse. Data points more than 2.5 standard deviations from the mean were removed. The remaining shots were averaged. The final time-wavelength data-set was generated from multiple data points at each pump-probe delay.

1.3 Magnetic Field Effects (MFE)

The photoluminescence intensity of V79 films were measured as a function of magnetic field strength using the method previously reported.[29] Briefly, the sample was placed in the field of an electromagnet (Magnetech MFG-6-24) and irradiated with a 532 nm diode laser (Thorlabs). The field was calibrated using a gauss meter (Lakeshore 475 DSP), with the applied current controlled by a Keithley 2230G-30-A power supply. The photoluminescence was detected using a diode array detector (Ocean Optics FLAME-S-XR1-ES).

1.4 Photoconductivity

Photoconductivity of drop-cast, room temperature V79 film was investigated using our home-built microwave absorption apparatus, detailed elsewhere.[30] Briefly, we monitored the change in reflected microwave power as a function of time after photoexcitation with a pulsed laser (Opolette 355).

2 Computational Methods

The structure of V79 was approximated as the methyl di-ester, the long hydrocarbon chains not being expected to impact the spectroscopic properties. The equilibrium geometries in the ground and lowest triplet states were obtained using the Gaussian 16 program,[31] at the ωB97x-D/6-31G(d) level of theory.[32, 33] At these geometries, vertical spectroscopic transitions were investigated by performing time-dependent density functional theory with the 6-311G(d) basis set.
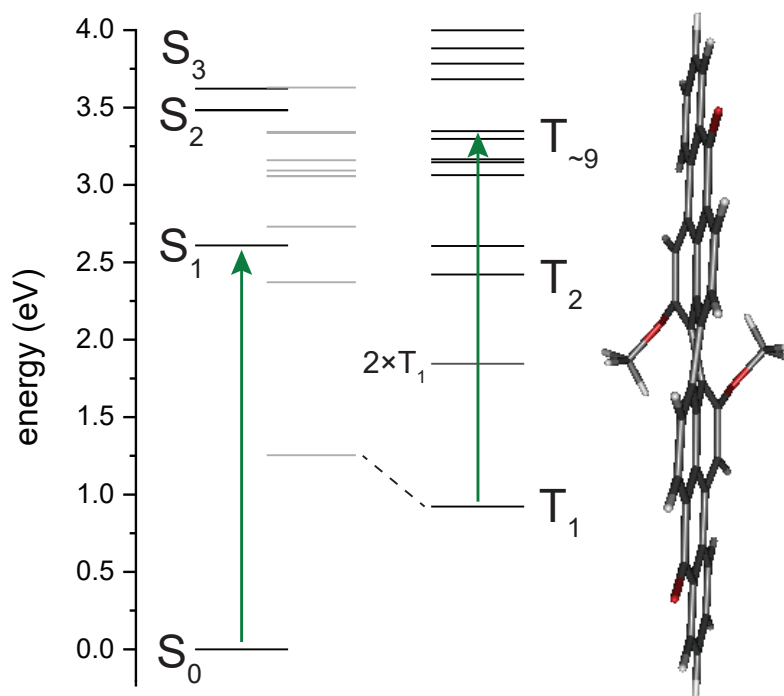
Figure 1: Left: Jablonski diagram calculated by TD-DFT. The relaxed T_1 energy is set empirically. The strong absorptions are indicated with vertical arrows. Right: The S_0 ωB97X-D/6-31G(d) geometry (C_2 symmetry).

3 Results

3.1 TD-DFT Calculations

The results of the TD-ωB97X-D/6-311G(d)//ωB97X-D/6-31G(d) calculations are reported in Table 1. At the ground state geometry (S_0, depicted in Figure 1), a strong transition at 2.6 eV with $f = 0.85$ is calculated to S_1, polarized perpendicularly to the C_2 symmetry axis. The unrelaxed T_1 state is computed by TD-DFT to be at 1.25 eV. A large number of triplet states are calculated, but notably at the relaxed T_1 geometry, a strong transition at 2.4 eV is calculated with $f = 0.82$, polarized in the same sense as the $S_1 \leftarrow S_0$ transition. The upper state of this transition is calculated to be T_9, but is more rigorously denoted $4\,^3A$.

The steady-state absorption spectrum of V79 is shown as the dashed curve in Figure 2. The strong absorption of V79 which corresponds to the predicted strong $S_1 \leftarrow S_0$ transition calculated to be at 2.6 eV is found at 2.0 eV. The breadth of the absorption band indicates that some of the disparity is due to a change in geometry between S_0 and S_1. Nevertheless, as will become apparent, it is important to note that TD-DFT predicts that both the S_0 and T_1 states exhibit transitions of similar strength at similar energies.

3.2 Single-component transient absorption

The transient absorption (TA) spectrum of dilute V79 in toluene was fit with a single exponential decay. The resulting spectrum is displayed in Figure 2. The comparison to the steady-state absorption indicates a stimulated emission feature at 1.84 eV and a broad ground-state bleach from about 1.9 eV upwards. A notable excited-state absorption is apparent at 1.11 eV. The decay was fit to a time constant of 4.97(17) ns.

The TA trace of dilute PtOEP in toluene is fit to a single spectrum, displayed in Figure 2. The standout feature is the bleach, which closely resembles the steady-state absorption spectrum. From the height of the bleach at 2.32 eV, we can calibrate the TA spectrum, resulting in an

Table 1: Transitions of the Violanthrone Chromophore Calculated at the TD-ωB97x-D/6-311G(d)//ωB97x-D/6-31G(d) Level of Theory.

| Lower State	Upper State	Γ_μ	Energy (eV)	Wavelength (nm)	f
S_0	T_1	B	1.2536	989	-
	T_2	A	2.3716	523	-
	S_1	B	2.6088	475	0.854
	T_3	B	2.7309	454	-
	T_4	B	3.0564	406	-
	T_5	A	3.0572	406	-
	T_6	A	3.0934	401	-
	T_7	B	3.1600	392	-
	T_8	B	3.3350	372	-
	T_9	A	3.3422	371	-
	S_2	A	3.4818	356	0.000
	S_3	B	3.4845	356	0.003
	S_4	A	3.6220	342	0.021
	T_{10}	A	3.6295	342	-
T_1	T_2	B	1.4989	827	0.017
	T_3	A	1.6830	737	0.001
	T_4	B	2.1407	579	0.036
	T_5	B	2.2239	558	0.0002
	T_6	A	2.2244	557	0.0002
	T_7	A	2.2427	553	0.045
	T_8	A	2.3752	522	0.047
	T_9	B	2.4251	511	0.820
	T_{10}	A	2.7604	449	0.025
	T_{11}	B	2.8616	433	0.187
	T_{12}	B	2.9601	419	0.0001
	T_{13}	A	3.0761	403	0.014
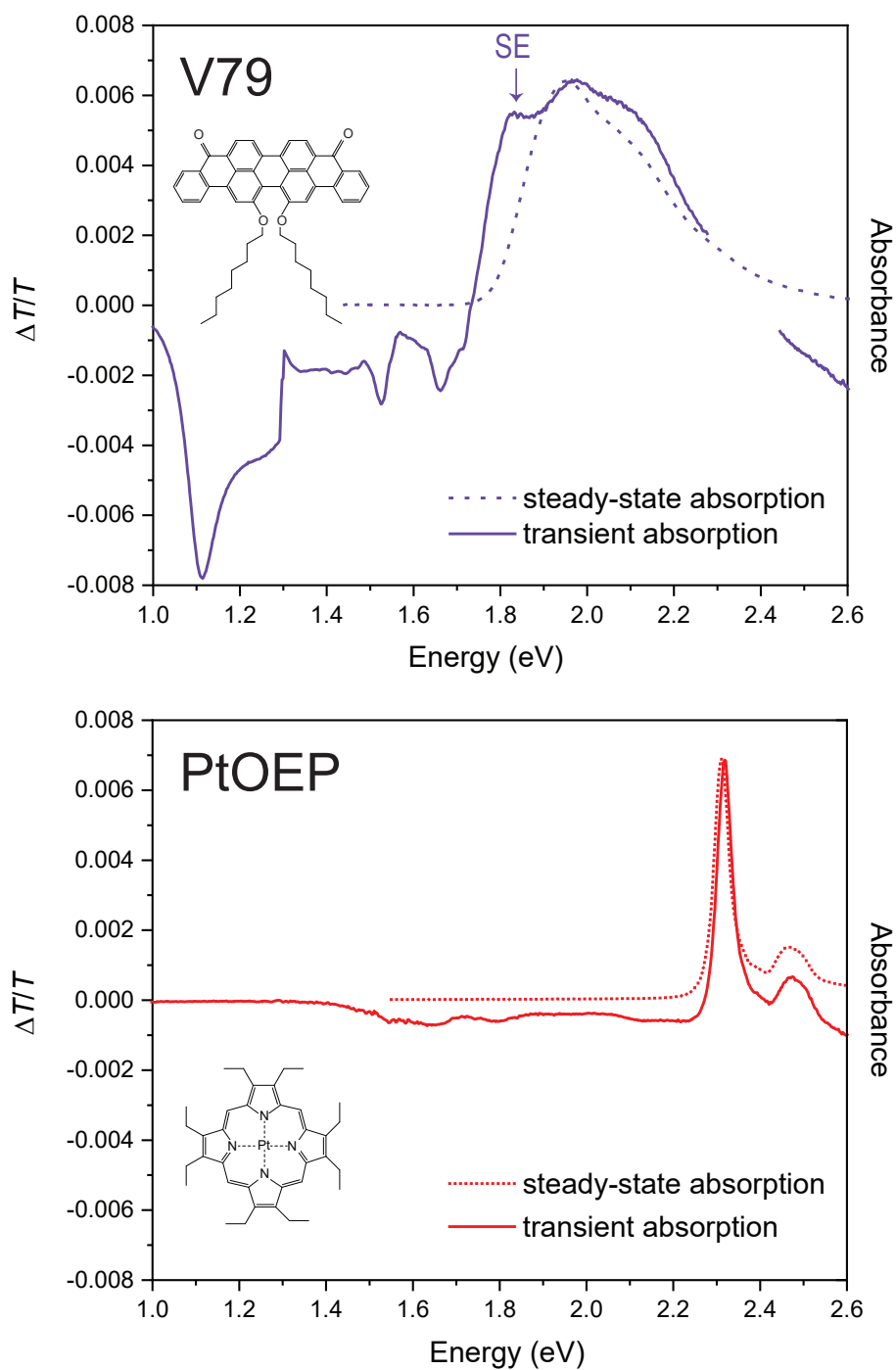
Figure 2: The transient spectra of [1]V79 and [3]PtOEP, compared to their steady-state absorption spectra (dashed lines). V79 clearly exhibits a stimulated emission (SE) feature at 1.84 eV.

absorption coefficient at $2.48\,\text{eV}$ of $572\,\text{M}^{-1}$ (1 mm pathlength). A fit to the TA spectrum reveals a lifetime of $338\,\mu\text{s}$, which is therefore attributed to ^{3}PtOEP. This accords with the absence of a stimulated emission feature.

3.3 Triplet Sensitization

The TA spectrum of the mixture of V79 and PtOEP in toluene is displayed in Figure 3. The data set was fit, resulting in decay-associated spectra corresponding to time constants of 6.7 ns, $1.04\,\mu\text{s}$ and $16.1\,\mu\text{s}$. Both species are excited by the 532 nm laser pulse. The first spectrum is identified with the excited singlet of V79. It does not exhibit any spectral correlations with the other components, and thus may be considered kinetically unconnected to the other species.

The spectrum of the $1.04\,\mu\text{s}$ decay is anticorrelated with the spectrum of the $16\,\mu\text{s}$ decay in the $1.8 - 2.2\,\text{eV}$ region, indicating that species are kinetically related. The $1.04\,\mu\text{s}$ spectrum exhibits the 2.48 eV (500 nm) shoulder of ^{3}PtOEP (Figure 2), allowing the TA spectrum of ^{3}PtOEP to be recovered from the sum of the $1.04\,\mu\text{s}$ and $16\,\mu\text{s}$ spectra. Triplet energy transfer from ^{3}PtOEP to ground state V79, yields ^{3}V79, which decays over $16\,\mu\text{s}$. The species-associated spectra are plotted in Figure 3.

The spectrum of ^{3}V79 hardly exhibits a bleach at all, which is ascribed to overlapping excited-state absorptions in the ground-state bleach region. As explained above, this is entirely consistent with the results of TD-DFT calculations. The transient absorption spectrum of ^{3}V79 was calibrated from the extinction of the Q-band bleach of ^{3}PtOEP and the triplet energy transfer yield, taken from the ^{3}PtOEP state lifetimes in the presence ($\tau_{^3PtOEP,q}$) and absence of V79 ($\tau_{^3PtOEP}$).

$$\Delta\varepsilon_{^3V79}(\lambda) = \frac{\Delta A_{^3V79}(\lambda)\Delta\varepsilon_{PtOEP}(500\,\text{nm})}{\Phi_{TET}\Delta A_{^3PtOEP}(500\,\text{nm})} \tag{1}$$
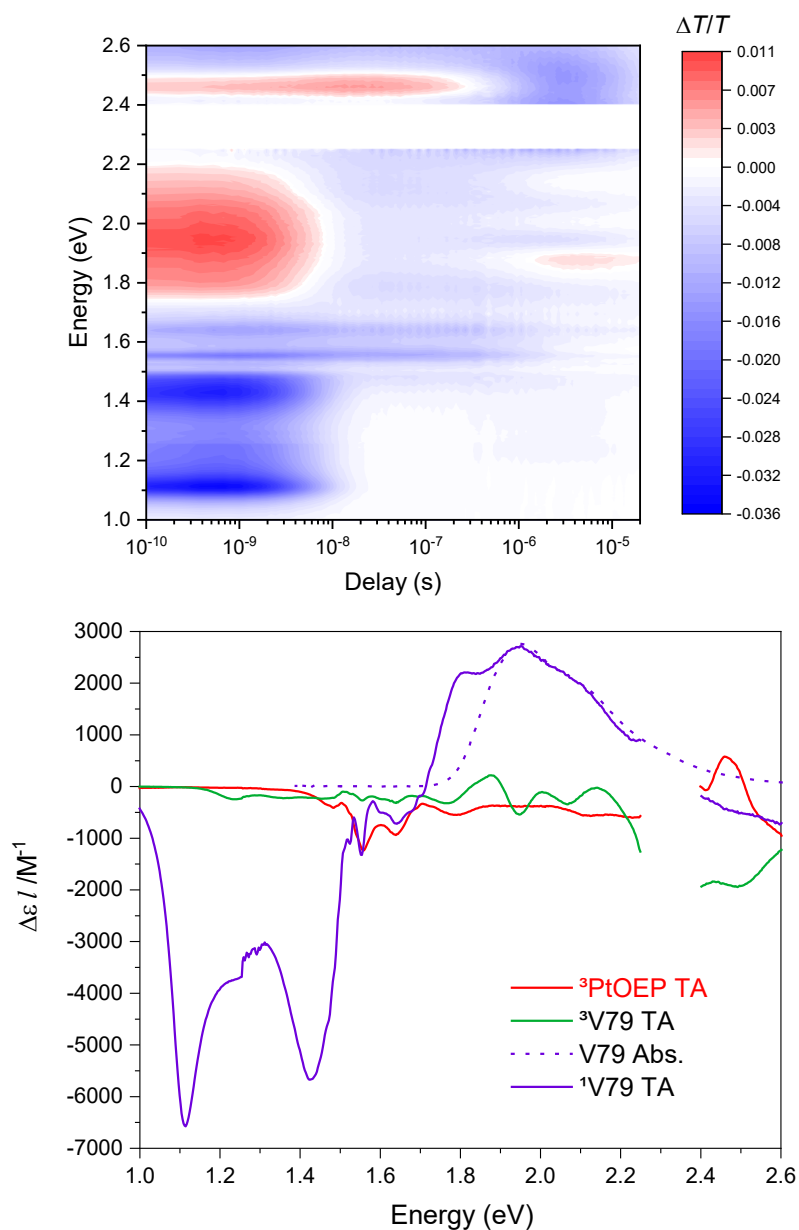
Figure 3: Top: The transient absorption spectrum of a mixture of V79 and PtOEP. Both species are excited by the 532 nm laser pulse, with the ^{1}V79 decaying on a nanosecond time-scale. The excited PtOEP undergoes intersystem crossing, resulting in long-lived ^{3}PtOEP which transfers energy to ground state V79 molecules resulting in ^{3}V79, which has a 16 μs lifetime. Bottom: The species-associated spectra.

$$\Phi_{TET} = 1 - \frac{\tau_{3\,PtOEP,q}}{\tau_{3\,PtOEP}} \tag{2}$$

3.4 Exciton dynamics in a V79 film

The TA spectrum of a drop-cast film of V79 is shown in Figure 4. There is a rapid decay evident on the few ps timescale, a ≈ 100 ps-lifetime species with a broad ground-state bleach, and a long-lived species with a narrow, red-shifted ground state bleach. The decay-associated spectra are shown at the bottom of Figure 4. There was no discernable effect on the observed emission due to magnetic fields (Figure 4). Reasons for this are discussed below.

4 Discussion

To interpret the decay-associated spectra in terms of species, we require a kinetic model. There are two distinct situations: a branching whereby an initial photo-generated species gives rise to two subsequent species in parallel, and a sequential model, where there is a linear progression of energy from one species to another via an intermediate.

If the spectra with 3.35 ps, 101 ps and 5.5 ns decays are denoted $\sigma_n (n = 1, 2, 3)$, then the expected species-associated spectra, $\sigma_\alpha (\alpha = A, B, C)$ are in the sequential case,

$$\sigma_A = \sigma_1 + \sigma_2 + \sigma_3$$

$$\sigma_{B_{seq.}} = \sigma_2 + \sigma_3$$

$$\sigma_C = \sigma_3$$

$$\tag{3}$$

In the parallel case, only σ_B is different,
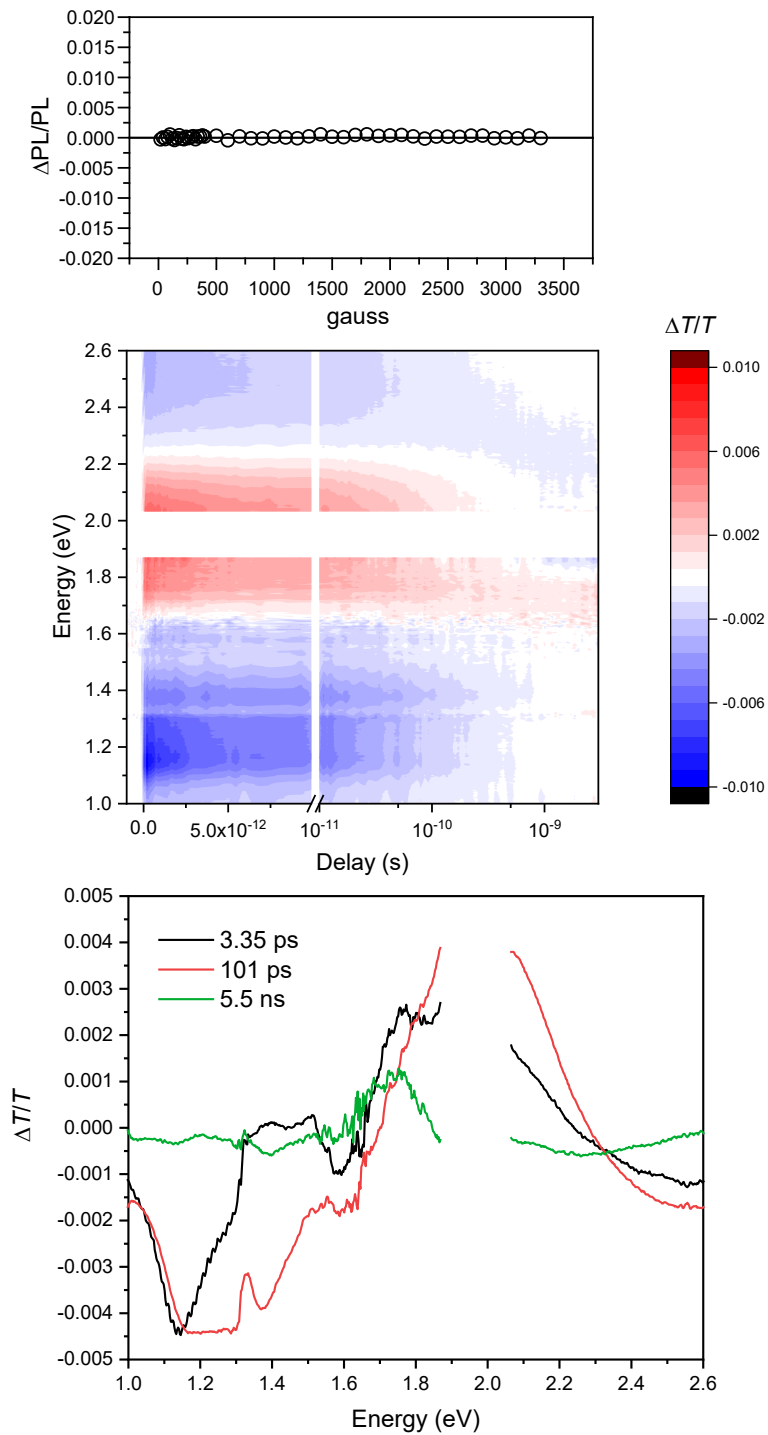
$$\sigma_{B_{||}} = \sigma_2$$

11

Figure 4: Top: Film luminescence as a function of magnetic field strength. Middle: The transient absorption of a drop-cast film of V79. Bottom: The decay-associated spectra.
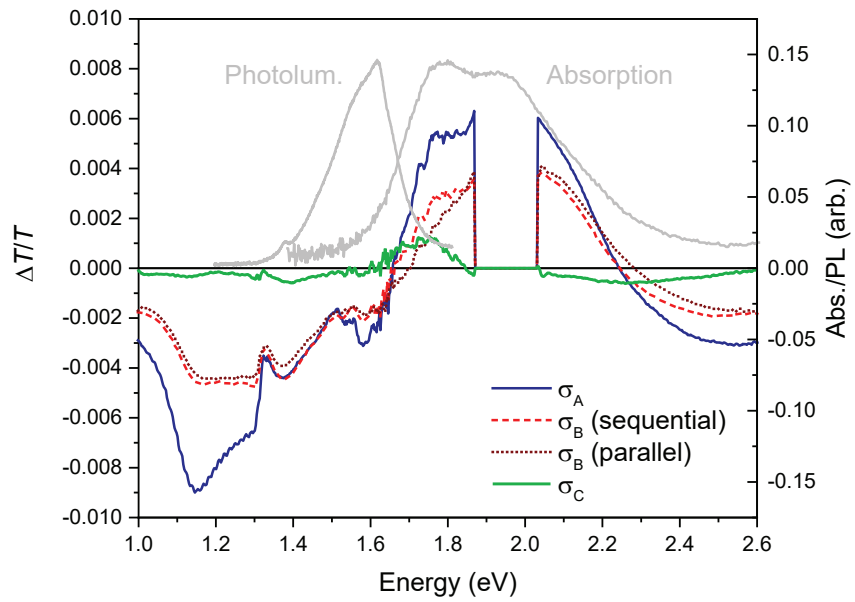
Figure 5: The species-associated spectra extracted from the data in Figure 4.

The species associated spectra are shown in Figure 5.

There is no difference in σ_A or σ_C in the models. It is expected that the initially prepared state will be the S_1 state of V79. Comparing σ_A to the transient V79 spectrum in Figure 2, we see that the bleach and the strong 1.1 eV excited-state absorption are accounted for. The absorption spectrum of the film, shown in Figure 5, is red-shifted compared to the solution, indicating excitonic coupling. Any stimulated emission feature is probably overlapped by an excited-state absorption.

It is tempting to attribute the final species represented by σ_C to the ^{3}V79 triplet. This could result from singlet fission of the ^{1}V79 state, and as shown in Figure 3, the triplet has extensive excited-state absorptions which mask the ground state bleach. Excitonic coupling in the solid could shift these absorptions compared to solution, resulting in a transient spectrum that differs. The small bleach rises from 1.55 eV, matching the low energy edge of the film absorption spectrum.

The possibility that a charge-transfer state is generated is not supported by calculations. A TD-ωB97X-D/6-311G(d)//ωB97X-D/6-31G(d) calculation of the V79 cation predicts a strong excitation ($f = 0.7$) at 2.0 eV. Given that the $S_1 - S_0$ transition was calculated too high by some 0.6 eV, it would be expected that the cation would absorb to lower energy than the calculated 2.0 eV and be evident in the transient absorption spectrum. Nevertheless, we note that films of violanthrone itself, which lacks the solubilizing octyloxy groups, photoconductivity is observed.[34] Attempts to observed photoconductivity in V79 were unsuccessful.

The choice of a sequential or parallel models comes down to a choice of σ_B spectrum. The sequential model appears to have a bleach which is the same shape as that in σ_A, closely matching the absorption spectrum. Conversely, the parallel σ_B spectrum has a diminished bleach around 1.75 eV. Another point in favour of the sequential model is the rate for generation of the putative triplet. It is expected that singlet fission is slightly endothermic in this case. As such,

a singlet lifetime of 3 ps would be unlikely. In the case of tetracene crystals, another endothermic fission system, the lifetime is hundreds of ps,[35] and even in films where the decay is to crystal defects, the decay is on the order of 100 ps.[36, 37] We thus attribute spectrum σ_B to an excitonically relaxed singlet which gives rise to triplets by endothermic singlet fission.

Magnetic fields are often used as a method to characterize singlet fission. It is well established that a pool of statistically populated triplets undergo inhibited triplet-triplet annihilation in magnetic fields, the effect usually being of the order of several percent at fields of 3000 G.[38] By the principle of detailed balance, one would therefore also expect the singlet fission process to produce a pool of statistical triplets to be hindered, and thus potentially enhanced photoluminescence would result. This has been observed in solution[39] and in the solid state.[3, 40]

However, a magnetic field enhancement of PL requires a *quasi*-equilibrium between the bright singlet state and the weakly-coupled triplet pair $((T...T))$.[41] This requires that the rate for reformation of the singlet state is comparable to or exceeds that of triplet dissociation (or decorrelation). The lack of a magnetic field effect here suggests that either this criteria is missing, or that singlet fission is not occuring. Since singlet fission here would be slightly endothermic, it is expected that population could indeed be exchanged between the S_1 and $(T...T)$ states. Tetracene, which is an endothermic singlet fission material, exhibits the characteristic effect.[3] However, if the dissociation of the $(T...T)$ state is rapid, all photoluminescence is detected on the first pass, and there would be no magnetic field effect observed. It may thus be concluded that the absence of a magnetic field effect does not rule out singlet fission in the same way that its presence would confirm it. No delayed fluorescence was observed.

It was noted that the fluorescence lifetime in the closely related V78 chromophore was as short as 20 ps.[25] V78 differs by having ester linkages where V79 has ether groups. It is thus likely that V78 also decays to a (pair of) triplet states by singlet fission. This underscores a general problem with performing triplet fusion upconversion in the condensed phase at finite

temperature. Even where singlet fission is endothermic, it likely has a rate that is faster than fluorescence, and is thus detrimental to the desired outcome. While this problem can be mitigated by doping, a more elegant approach would be to engineer the electronic coupling between chromophores to tune the singlet fission (and thus also triplet fusion) rate well below the fluorescence rate. Since the triplet lifetime exceeds the fluorescence lifetime by orders of magnitude, such an approach would seem plausible.

5 Conclusions

The transient absorption spectra of V79 and PtOEP were studied separately, and used determine that the transient absorption spectrum of $^3V79$ has a ground-state bleach which is largely balanced by excited state absorption. This was supported by the results of time-dependent density functional theory.

In V79 films, the excited singlet state is found to live only about $100\,\mathrm{ps}$ before decaying to a triplet state, as evidenced by the lack of a strong ground-state bleach and the longevity of the terminal electronic state. The absence of intersystem crossing identified in solution and the demonstration that V79 undergoes TTA strongly suggest that in the film it is undergoing endothermic singlet fission. Attempts to conclusively show this with magnetic field effects were unsuccessful.

Data Availability

The data that support the findings of this study are available from the corresponding author upon reasonable request.

Acknowledgements

References

[1] Schulze, T. F. & Schmidt, T. W. Photochemical upconversion: present status and prospects for its application to solar energy conversion. *Ener. Environ. Sci.* **8**, 103–125 (2015).

[2] Zhou, Y., Ruchlin, C., Robb, A. J. & Hanson, K. Singlet sensitization-enhanced upconversion solar cells via self-assembled trilayers. *ACS Energy Lett.* **4**, 1458–1463 (2019).

[3] Einzinger, M. *et al.* Sensitization of silicon by singlet exciton fission in tetracene. *Nature* **571**, 90–94 (2019).

[4] MacQueen, R. W. *et al.* Crystalline silicon solar cells with tetracene interlayers: the path to silicon-singlet fission heterojunction devices. *Mater. Horiz.* **5**, 1065–1075 (2018).

[5] Rao, A. & Friend, R. H. Harnessing singlet exciton fission to break the shockley–queisser limit. *Nat. Rev. Mater.* **2**, 17063 (2017).

[6] Tayebjee, M. J. Y., McCamey, D. R. & Schmidt, T. W. Beyond shockley–queisser: Molecular approaches to high-efficiency photovoltaics. *J. Phys. Chem. Lett.* **6**, 2367–2378 (2015).

[7] Jiang, Y. *et al.* Singlet fission and tandem solar cells reduce thermal degradation and enhance lifespan. *Prog. Photovolt.* (2021).

[8] Ravetz, B. D. *et al.* Photoredox catalysis using infrared light via triplet fusion upconversion. *Nature* **565**, 343–346 (2019).

[9] Khnayzer, R. S. *et al.* Upconversion-powered photoelectrochemistry. *Chem. Commun.* **48**, 209–211 (2012).

[10] Bonnet, S. Shifting the light activation of metallodrugs to the red and near-infrared region in anticancer phototherapy. *Comm. Inorg. Chem.* **35**, 179–213 (2015).

[11] Zhou, J., Liu, Q., Feng, W., Sun, Y. & Li, F. Upconversion luminescent materials: Advances and applications. *Chem. Rev.* **115**, 395–465 (2015).

[12] Wen, S. *et al.* Future and challenges for hybrid upconversion nanosystems. *Nat. Photon.* **13**, 828–838 (2019).

[13] Pedrini, J. & Monguzzi, A. Recent advances in the application triplet–triplet annihilation-based photon upconversion systems to solar technologies. *J. Photon. Ener.* **8**, 8 – 8 – 16 (2017).

[14] Schmidt, T. W. & Castellano, F. N. Photochemical upconversion: the primacy of kinetics. *J. Phys. Chem. Lett.* **5**, 4062–4072 (2014).

[15] Bharmoria, P., Bildirir, H. & Moth-Poulsen, K. Triplet–triplet annihilation based near infrared to visible molecular photon upconversion. *Chem. Soc. Rev.* **49**, 6529–6554 (2020).

[16] Smith, M. B. & Michl, J. Singlet fission. *Chem. Rev.* **110**, 6891–6936 (2010).

[17] Smith, M. B. & Michl, J. Recent advances in singlet fission. *Ann. Rev. Phys. Chem.* **64**, 361–386 (2013).

[18] Congreve, D. N. *et al.* External quantum efficiency above 100% in a singlet-exciton-fission–based organic photovoltaic cell. *Science* **340**, 334–337 (2013).

[19] Ehrler, B., Wilson, M. W. B., Rao, A., Friend, R. H. & Greenham, N. C. Singlet exciton fission-sensitized infrared quantum dot solar cells. *Nano Letters* **12**, 1053–1057 (2012).

[20] Tritsch, J. R., Chan, W.-L., Wu, X., Monahan, N. R. & Zhu, X. Harvesting singlet fission for solar energy conversion via triplet energy transfer. *Nature Commun.* **4**, 2679 (2013).

[21] Jadhav, P. J., Mohanty, A., Sussman, J., Lee, J. & Baldo, M. A. Singlet exciton fission in nanostructured organic solar cells. *Nano Letters* **11**, 1495–1498 (2011).

[22] Tayebjee, M. J. Y., Gray-Weale, A. A. & Schmidt, T. W. Thermodynamic limit of exciton fission solar cell efficiency. *J. Phys. Chem. Lett.* **3**, 2749–2754 (2012).

[23] Fückel, B. *et al.* Singlet oxygen mediated photochemical upconversion of nir light. *J. Phys. Chem. Lett.* **2**, 966–971 (2011).

[24] Gholizadeh, E. M. *et al.* Photochemical upconversion of near-infrared light from below the silicon bandgap. *Nat. Photonics* **14**, 585–590 (2020).

[25] Kakuichi, M., Kasatani, K. & Morita, Y. Preparation of nanoparticles of a violanthrone derivative with properties of j-like aggregates. *Trans. Mat. Res. Soc. Japan* **37**, 471–474 (2012).

[26] Wu, M. *et al.* Solid-state infrared-to-visible upconversion sensitized by colloidal nanocrystals. *Nat. Photonics* **10**, 31–34 (2016).

[27] Wieghold, S., Bieber, A. S., Van Orman, Z. A., Rodriguez, A. & Nienhaus, L. Is disorder beneficial in perovskite-sensitized solid-state upconversion? the role of dbp doping in rubrene. *J. Phys. Chem. C* **124**, 18132–18140 (2020).

[28] Penconi, M., Gentili, P. L., Massaro, G., Elisei, F. & Ortica, F. A triplet–triplet annihilation based up-conversion process investigated in homogeneous solutions and oil-in-water microemulsions of a surfactant. *Photochem. Photobiol. Sci.* **13**, 48–61 (2014).

[29] Gao, C. *et al.* Intramolecular versus intermolecular triplet fusion in multichromophoric photochemical upconversion. *J. Phys. Chem. C* **123**, 20181–20187 (2019).

[30] Guse, J. A. *et al.* Spectral dependence of direct and trap-mediated recombination processes in lead halide perovskites using time resolved microwave conductivity. *Phys. Chem. Chem. Phys.* **18**, 12043–12049 (2016).

[31] Frisch, M. J. *et al.* Gaussian 16 RevisionC.01 (2016). Gaussian Inc. Wallingford CT.

[32] Chai, J.-D. & Head-Gordon, M. Long-range corrected hybrid density functionals with damped atom–atom dispersion corrections. *Phys. Chem. Chem. Phys.* **10**, 6615–6620 (2008).

[33] Krishnan, R., Binkley, J. S., Seeger, R. & Pople, J. A. Self-consistent molecular orbital methods. XX. a basis set for correlated wave functions. *J. Chem. Phys.* **72**, 650–654 (1980).

[34] Akamatu, H. & Inokuchi, H. Photoconductivity of violanthrone. *J. Chem. Phys.* **20**, 1481–1483 (1952).

[35] Piland, G. B. & Bardeen, C. J. How morphology affects singlet fission in crystalline tetracene. *J. Phys. Chem. Lett.* **6**, 1841–1846 (2015).

[36] Burdett, J. J., Gosztola, D. & Bardeen, C. J. The dependence of singlet exciton relaxation on excitation density and temperature in polycrystalline tetracene thin films: Kinetic ev-

idence for a dark intermediate state and implications for singlet fission. *J. Chem. Phys.* **135**, 214508 (2011).

[37] Tayebjee, M. J. Y., Clady, R. G. C. R. & Schmidt, T. W. The exciton dynamics in tetracene thin films. *Phys. Chem. Chem. Phys.* **15**, 14797–14805 (2013).

[38] Merrifield, R. E. Theory of magnetic field effects on the mutual annihilation of triplet excitons. *J. Chem. Phys.* **48**, 4318–4319 (1968).

[39] Thompson, N. J., Hontz, E., Chang, W., Van Voorhis, T. & Baldo, M. Magnetic field dependence of singlet fission in solutions of diphenyl tetracene. *Phil. Trans. Roy. Soc. A* **373** (2015).

[40] Groff, R., Avakian, P. & Merrifield, R. Magnetic field dependence of delayed fluorescence from tetracene crystals. *J. Luminesc.* **1-2**, 218 – 223 (1970).

[41] Burdett, J. J., Piland, G. B. & Bardeen, C. J. Magnetic field effects and the role of spin states in singlet fission. *Chem. Phys. Lett.* **585**, 1–10 (2013).